

Critical behavior of the $S=1/2$ Heisenberg ferromagnet: A Handscomb quantum Monte Carlo study

Adauto J. F. de Souza

*Departamento de Física e Matemática, Universidade Federal Rural de Pernambuco, 52171-030 Recife PE, Brazil
and Departamento de Física, Universidade Federal de Pernambuco, 50607-901 Recife - PE, Brazil*

U. M. S. Costa

Departamento de Física, Universidade Federal do Ceará, 60470-455 Fortaleza - CE, Brazil

M. L. Lyra

Departamento de Física, Universidade Federal de Alagoas, 57072-970 Maceió - AL, Brazil

(Received 11 April 2000)

We investigate the critical relaxational dynamics of the $S=1/2$ Heisenberg ferromagnet on a simple cubic lattice within the Handscomb prescription, on which a diagrammatic series expansion of the partition function is computed by means of a Monte Carlo procedure. Using a phenomenological renormalization-group analysis of graph quantities related to the spin susceptibility and order parameter, we obtain precise estimates of the critical exponents relations $\gamma/\nu=1.98\pm 0.01$ and $\beta/\nu=0.512\pm 0.002$ and of the Curie temperature $k_B T_c/J=1.6778\pm 0.0002$. The critical correlation time τ_{int} of both energy and susceptibility is also computed. We found the number of Monte Carlo steps needed to generate uncorrelated diagram configurations scales with the system's volume. We estimate the efficiency of the Handscomb method, comparing its ability in dealing with the critical slowing down to that of other quantum and classical Monte Carlo prescriptions.

I. INTRODUCTION

The slowing down of the relaxation to thermal equilibrium is an important physical phenomenon associated with the build up of long-range correlations at the critical point of spin systems. According to the finite-size scaling hypothesis, the critical relaxation time scales with the system size as $\tau \propto L^z$, with the dynamical critical exponent z governing the rate of convergence towards thermal equilibrium. The value of z depends on the particular equation of motion of the order parameter and of the conservation laws that apply to the spin system. In particular, the dynamic scaling theory predicts that for the classical isotropic Heisenberg model with conserved order parameter $z=d-\beta/\nu$ ($z\sim 2.5$ for $d=3$),¹ which is consistent with both experiments^{2,3} and numerical simulations.⁴ For a recent review see Ref. 5.

Monte Carlo simulation is a powerful tool to study the equilibrium properties of a spin system through some stochastic relaxational dynamics. It defines a Markovian process in which the associated stochastic model evolves in the phase space according to certain transition probabilities. The transition rates between two distinct spin configurations are imposed to satisfy the detailed balance condition in order to lead the system to its equilibrium state distribution. The dynamical evolution of the stochastic model can be thought of resulting from the interactions among its many degrees of freedom. However, the evolution of the model system under the Monte Carlo dynamics do not need to be consistent with any motion equation. In this context, the critical exponent z characterizes, therefore, the rate at which a particular set of stochastic dynamical rules generates uncorrelated spin configurations.

A general feature of Monte Carlo simulations of classical

spin models is that cluster dynamics are usually much more effective in overcoming the critical slowing down than those which are based on single spin-flip procedures. For example, the cluster Monte Carlo algorithm introduced by Swendsen-Wang⁶ is known to have a very fast convergence to equilibrium at the critical point in contrast to the slower convergence of local dynamics such as Metropolis and heat-bath. For the isotropic classical Heisenberg model it has been found that $z\sim 2$ for Metropolis⁷ and $z\sim 0$ for the single cluster^{8,9} Monte Carlo dynamics.

The traditional spin-flip Monte Carlo algorithms as applied to classical spin systems can not be directly extended to quantum spin models. The problem resides in the fact that the Hamiltonian is not, in general, diagonal in the spin configuration basis. A quantum Monte Carlo method was introduced by Handscomb for the calculation of the thermodynamical properties of quantum Heisenberg ferromagnets.¹⁰ The main difference of this technique in comparison to traditional Monte Carlo algorithms is that the sample space is not related to any kind of physical phase space. It is the diagrammatic series of the partition function that is calculated by means of the Monte Carlo method. The Handscomb method has been successfully used to compute the thermodynamical properties of the Heisenberg $S=1/2$ ferromagnet¹¹⁻¹⁴ and extended to a form applicable to a series of quantum spin models.¹⁵

Another algorithm commonly used in Monte Carlo simulations of quantum spin models is based on the use of the generalized Trotter formula to map the quantum system onto a classical system with an additional imaginary time dimension.¹⁶ The $S=1/2$ Heisenberg model has been extensively studied within this line. Recently, a decoupled cell method for quantum Monte Carlo based on the Suzuki-

Trotter approach has been used to compute the critical dynamical exponent z of the $S=1/2$ Heisenberg model on the simple cubic lattice.¹⁷ It was found that $z \sim 2$ which is quite similar to the value obtained from simulations of the classical Heisenberg model under Metropolis dynamics.⁷

In the present work, we are going to investigate both the static and dynamic critical properties of the $S=1/2$ Heisenberg ferromagnet on the simple cubic lattice by means of the Handscomb dynamics. We will employ a phenomenological renormalization group to obtain precise estimates of the critical temperature and some static critical exponents. By employing a so-called moving block bootstrap (MBB) technique,¹⁸ we are going to calculate the equilibrium relaxation time for the energy and susceptibility at criticality. The critical time-displaced equilibrium correlation function will be computed as well. We will employ a finite-size scaling analysis of the equilibrium relaxation time to obtain the critical dynamical exponent z associated to the Handscomb dynamics and we contrast it with the results from the quantum decoupled cell method and the results from distinct Monte Carlo simulations of the classical Heisenberg model.

II. THE HANDSCOMB MONTE CARLO METHOD

Let us briefly draw the main ideas of the Handscomb method. Consider the Hamiltonian of a quantum spin system to be given by

$$H = \sum_i^{N_0} H_i, \quad [H_i, H_j] \neq 0. \quad (1)$$

The canonical average of a physical observable A can be expanded in the form

$$\langle A \rangle = \frac{\text{Tr}[A \exp(-\beta H)]}{\text{Tr}[\exp(-\beta H)]} = \sum_r \sum_{C_r} A(C_r) p(C_r), \quad (2)$$

where $\beta = 1/k_B T$, \sum_{C_r} denotes a summation over all ordered sets of indices $C_r \equiv \{i_1, i_2, \dots, i_r\}$ (Mayer diagrams) and

$$A(C_r) \equiv \frac{\text{Tr}[A H_{i_1} \cdots H_{i_r}]}{\text{Tr}[H_{i_1} \cdots H_{i_r}]},$$

$$p(C_r) \equiv \frac{\frac{(-\beta)^r}{r!} \text{Tr}[H_{i_1} \cdots H_{i_r}]}{\sum_r \sum_{C_r} \frac{(-\beta)^r}{r!} \text{Tr}[H_{i_1} \cdots H_{i_r}]}.$$
 (3)

Once $p(C_r) \geq 0$, it can be considered as a probability distribution and the canonical averages can be written as $\langle A \rangle = \langle A(C_r) \rangle_{p(C_r)}$. This is the case of the Heisenberg $S=1/2$ ferromagnet. The Hamiltonian can be represented in terms of transposition operators as

$$H = -J \sum E_{i,j}, \quad (4)$$

so that the relevant trace to be computed is that of a permutation operator

$$\text{Tr} P(C_r) \equiv \text{Tr}[E_{(i,j)_1} E_{(i,j)_2} \cdots E_{(i,j)_r}] = 2^{k(C_r)}, \quad (5)$$

where $k(C_r)$ is the number of cycles in the irreducible representation of the permutation $P(C_r)$. It is straightforward to show that any physical observable can be expressed in terms of the diagram structure. For instance, the internal energy is related to the average number of transposition operators in the diagrams and the susceptibility to the average size of the cycles in the diagram's irreducible representation.¹⁹

The Handscomb Monte Carlo method organizes a random walk in the space of the diagrams C_r which has $p(C_r)$ as the limit distribution. The dynamics suggested by Handscomb consists of three types of steps: (i) Step forward, chosen with probability f_r , which tries to include a randomly chosen bond to the right of the permutation operator; (ii) Step backwards, chosen with probability $1 - f_r$, which tries to remove a bond from the left of $P(C_r)$; (iii) cyclic transposition, chosen when step backwards is rejected, which moves a bond from the left to the right. The transition probabilities for performing each movement on the space of Mayer's diagrams are chosen in order to satisfy the detailed balance condition.

After a single step of the Handscomb Monte Carlo dynamics, the irreducible representation of the sequence C_r can have its cycle structure changed considerably. When two sites belong to distinct cycles, the insertion of the corresponding bond results in the coalescence of the two cycles of permutations. On the other hand, i.e., when the sites belong to the same cycle, the insertion breaks the cycle in two new ones. The same process occurs when a bond is removed from the sequence. Therefore, entire sets of sites can have their status changed during a single Monte Carlo step and, in this sense, the Handscomb dynamics is similar to the classical Monte Carlo cluster algorithms.

III. FINITE SIZE SCALING FOR THE SUSCEPTIBILITY AND ORDER PARAMETER

The susceptibility per spin of the quantum $S=1/2$ Heisenberg model is written in terms of the cyclic structure of the irreducible representation of C_r as¹⁹

$$\beta \chi = \frac{1}{N} \left\langle \sum_{j=1}^{k(C_r)} a_j^2 \right\rangle_P, \quad (6)$$

where a_j is the length of the j th cycle of the permutation $P(C_r)$ and $\langle \cdots \rangle_P$ denotes an average with respect to the C_r -space probability distribution. In Fig. 1, we show our results for the susceptibility from lattices of L^3 spins with $L=16, 24$, and 32 . In these simulations $150L^3$ Monte Carlo steps (insertion, removal or bond permutation) were enough to let the system evolve to an equilibrium diagram configuration starting from an initial diagram containing no transpositions. After equilibrium was reached, we averaged over 2×10^4 distinct diagrams, 10^3 MCS apart. These results were averaged over 10 distinct realizations of the numerical experiment. The susceptibility exhibits a critical behavior around $k_B T_c / J \approx 1.68$ in agreement with previous Monte Carlo estimates.²⁰ For $T > T_c$, χ is only weakly dependent on the system size; whereas it is nearly proportional to L^3 at low temperatures. Notice that χ equals the magnetization second moment for temperatures below T_c once the magnetization is strictly zero within the Handscomb prescription.

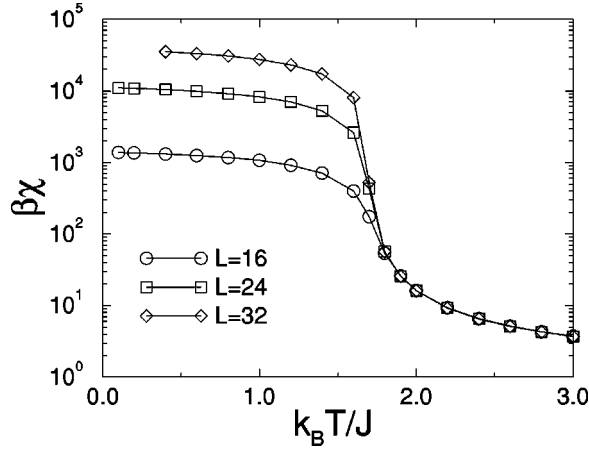


FIG. 1. The susceptibility per spin as a function of temperature for $L=16, 24$, and 32 (from below). Due to an intrinsic symmetry of the Handscomb dynamics, the susceptibility equals the magnetization second moment below T_c . The errors are much smaller than the size of the symbols.

In order to obtain a precise estimate of the critical temperature, we implemented a phenomenological renormalization-group analysis of the data from finite size lattices as introduced by Nightingale.²¹ The basic assumption is that near the transition the susceptibility of a finite lattice of linear size L scales as

$$\chi(T, L) = L^{\gamma/\nu} f_{\pm}(tL^{1/\nu}), \quad (7)$$

where $t = |(T - T_c)/T_c|$ and (\pm) stands for distinct scaling functions above and below T_c . The renormalization of temperature is defined by the following transformation relating lattices of two different sizes, L and L' :

$$\chi(T, L) = (L/L')^{\gamma/\nu} \chi(T', L') \quad (8)$$

with the fixed point giving T_c . Then a set of auxiliary functions is introduced as

$$g_{\chi}(T, L, L') = \frac{\ln[\chi(T, L)/\chi(T, L')]}{\ln(L/L')} \quad (9)$$

and these intersect as a function of temperature at a common point from which we can directly measure T_c and $\gamma/\nu = g_{\chi}(T_c, L, L')$. In Fig. 2 we plot the auxiliary functions $g_{\chi}(T, L, L')$ for typical renormalizations. Using all possible renormalizations with lattice sizes $L=16, 24, 32, 40$, and 48 , we estimate $k_B T_c/J = 1.677 \pm 0.001$ and $\gamma/\nu = 1.98 \pm 0.01$. These values are one order of magnitude more accurate than the previous Monte Carlo estimates from simulations on small lattices ($L \leq 10$) which reported $k_B T_c/J = 1.68 \pm 0.01$.²⁰

An even more accurate value for the critical temperature can be found by employing a renormalization study of critical quantities which are known to depict smaller fluctuations near the critical point such as the magnetization itself. Unfortunately, as we mention before, the magnetization is exactly zero for all temperatures due to an intrinsic symmetry of the Handscomb dynamics. However, we can explore the cycle structure of the Mayer diagrams to introduce a graph quantity which display the same critical behavior of the order

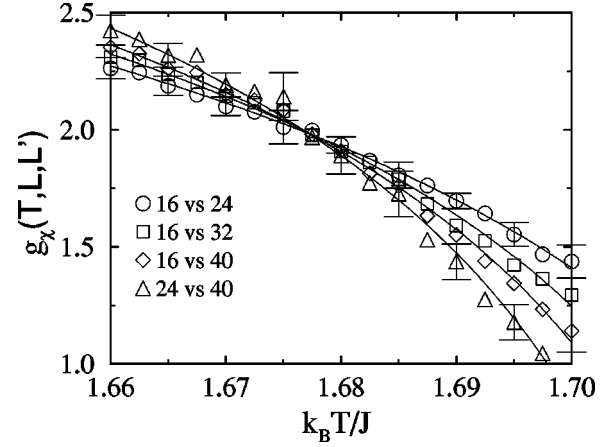


FIG. 2. The auxiliary functions $g_{\chi}(T, L, L')$ for the scaling of susceptibility data. The renormalizations were performed from $L=24$ to $L'=16$ (circles); $L=32$ to $L'=16$ (squares); $L=40$ to $L'=16$ (diamonds), and from $L=40$ to $L'=24$ (triangles). Typical error bars are shown. The solid lines are the results from renormalizations of the best fits of our original susceptibility data. These have a common point from which we estimate $T_c = 1.677 \pm 0.001$ and $\gamma/\nu = 1.98 \pm 0.01$.

parameter. In the simulations of classical spin models, such a quantity is the size of the largest cluster of spins which are in the same state. This might suggest that the largest cycle within a diagram in the context of Handscomb MC, may exhibit the same scaling behavior as the magnetization. Therefore, we will introduce a graph order parameter as the average size of the largest cycle of permutations.

In Fig. 3, we plot the average size of the largest cycle (normalized by the total number of sites) as a function of temperature from simulations on lattices with $L=16, 24$, and 48 . From this figure, one can see that the average size of the largest cycle depicts an overall behavior similar to the one expected for an order parameter, and it will be considered as a true order parameter from here on. It also indicates a phase

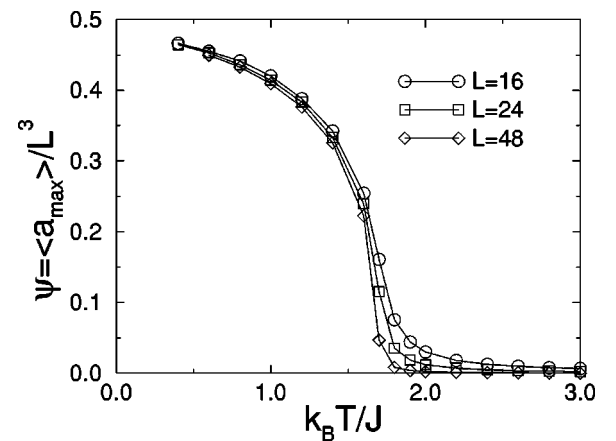


FIG. 3. The average size of the largest cycle (normalized the total number of sites) ψ as a function of temperature for $L=16, 24$, and 48 . At high temperatures all cycles are small indicating no long-range order and Ψ vanishes. With lowering T , the onset of the ferromagnetic order makes itself felt around $k_B T_c/J \approx 1.68$, and ψ start to grow until saturation. At criticality, ψ shows power-law size dependence.

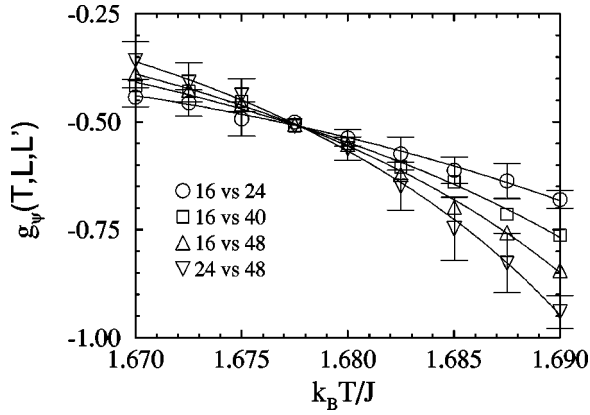


FIG. 4. The auxiliary functions $g_\psi(T, L, L')$ for the scaling of the order parameter data. The renormalizations were performed from $L=24$ to $L'=16$ (circles); $L=40$ to $L'=16$ (squares); $L=48$ to $L'=16$ (triangles up) and from $L=48$ to $L'=24$ (triangles down). Typical error bars are shown. The solid lines are the results from renormalizations of the best fit of our original order parameter data. From the interception of these functions computed for all possible renormalizations with lattice sizes $L=16, 24, 32, 40$, and 48 we estimate $k_B T_c / J = 1.6778 \pm 0.0002$ and $\beta/\nu = 0.512 \pm 0.002$.

transition around $k_B T_c / J \approx 1.68$. A renormalization analysis performed on the order parameter data is shown in Fig. 4. From these data we found $k_B T_c / J = 1.6778 \pm 0.0002$ and $\beta/\nu = 0.512 \pm 0.002$. To the best of our knowledge, the presently reported values for $k_B T_c / J$, γ/ν and β/ν are the most accurate Monte Carlo estimates to date for the quantum 3D Heisenberg ferromagnet. Our quoted value for T_c is in complete agreement with the most accurate high-temperature series study which yielded $J/k_B T_c = 0.5960(5)$.²² The critical exponents are in excellent agreement with the best estimates for the classical Heisenberg ferromagnet.²³

IV. CRITICAL RELAXATION OF THE SPIN-1/2 HEISENBERG MODEL

The critical relaxation within the Handscomb prescription can be investigated by computing some equilibrium time-displaced correlation functions $C(t)$ at the Curie temperature. We look at the equilibrium relaxation time τ which is expected to depict a power-law increase with the system size L whose exponent characterizes the critical relaxation process. In particular, it governs the size dependence of the rate at which uncorrelated configurations are generated during the Monte Carlo temporal evolution in phase space.

The fast growth of the relaxation time is referred to as the critical slowing down which may be governed by several relaxation modes.²⁴ One generally is interested in the slower relaxation modes, i.e., the longest relaxation times. Therefore, it is safer to work with the integrated correlation time given by

$$\tau_{int} = \int_0^\infty C(t) dt. \quad (10)$$

In order to estimate τ_{int} , we perform a very long MC simulation on L^3 simple cubic lattices, with $L = 16, 20, 24, 28, 32, 36, 40, 44, 48$, at the previously calculated critical temperature $k_B T_c / J = 1.6778$. The simulation is

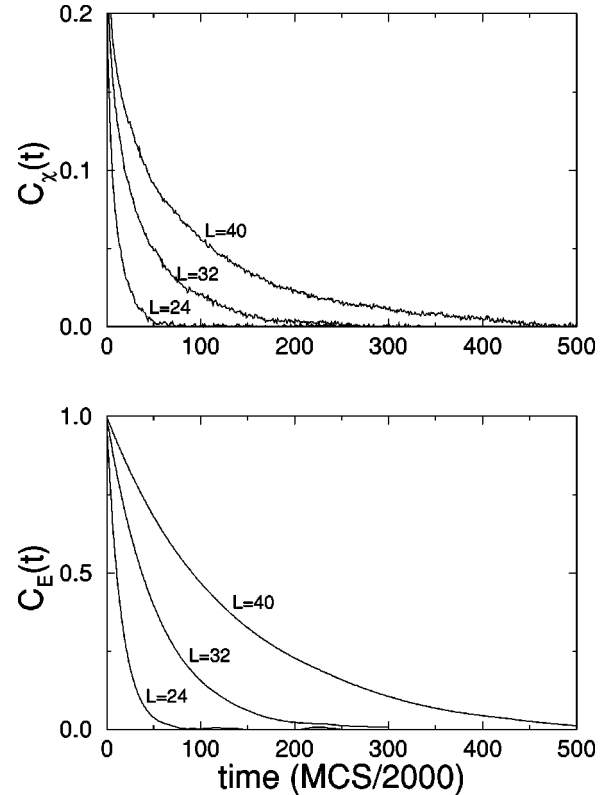


FIG. 5. The time-displaced equilibrium correlation function of the susceptibility and energy at criticality for several lattice sizes.

started from a diagram containing no transposition and we observed that typically $150L^3$ configurations were needed to bring the system to equilibrium. So we discarded the appropriate number of configurations for equilibration, after which we recorded the susceptibility and energy every $\delta t = 2000$ MCS, generating long equilibrium time series of 10^6 measurements each.

The time-displaced correlation functions (see Fig. 5) were obtained by $C_q(t) = \Delta_q(t) / \Delta_q(0)$, where $\Delta_q(t)$ is the autocovariance function given by

$$\Delta_q(t) = \frac{1}{n-t} \sum_{i=1}^{n-t} (q_i - \langle q \rangle)(q_{i+t} - \langle q \rangle), \quad (11)$$

n is the length of the time series, and q represents the physical property one is interested in.

Here, we computed $C_\chi(t)$ and $C_E(t)$, the correlation function of the susceptibility and energy, respectively. Typical equilibrium traces of the susceptibility and energy are shown in Fig. 6, where the microscopic time scale used equals 2000 MCS. From these we can infer that the number of MCS needed to generate two diagram configurations with uncorrelated susceptibilities is much smaller than the one required to generate uncorrelated energies.

In practice, τ_{int} was estimated by

$$\tau_{int} = \sum_{t=0}^{\infty} C_q(t) \quad (12)$$

and the sum was cut off at the first negative value of $C(t)$.

Despite our long runs we were not able to get reliable estimates of τ_{int} by integrating $C(t)$ for the largest lattices

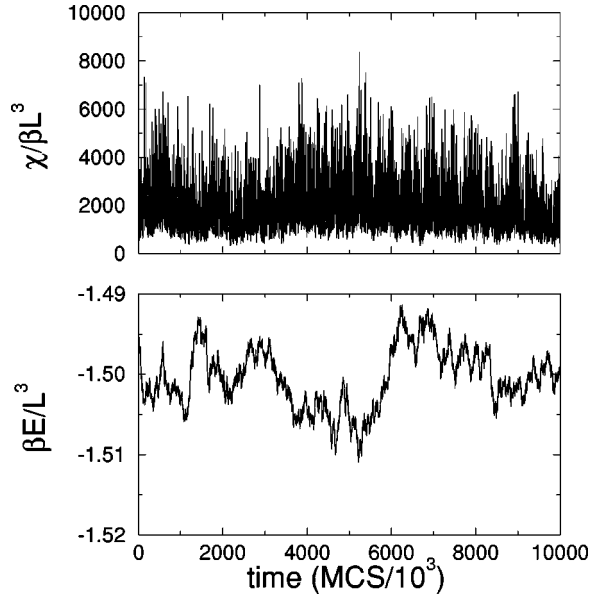


FIG. 6. An equilibrium trace of the susceptibility χ and energy E at criticality. Local quantities, as energy, are more time correlated than nonlocal ones due to the cluster nature of the Handscomb Monte Carlo method.

simulated. It is well known that $C(t)$ fluctuates wildly for large t , hampering the convergence of its integral.

On the other hand, in the context of MC simulations the error associated with a given quantity can be written as²⁵

$$\sigma^2 = \sigma_0^2 \left(1 + \frac{2\tau}{\delta t} \right), \quad (13)$$

where σ_0 is the standard deviation treating all data as if they were statistically independent and σ is the actual statistical uncertainty. This variance inflation correctly takes into account the correlations of the MC data.

It is not a simple matter to access the actual error in a finite time series of correlated data. Here we employed the moving block bootstrap (MBB) method,¹⁸ which exploits resampling techniques. Within the MBB scheme a block of observations is defined by its length and by its starting point in the series. For instance, $Q_i = \{q_i, q_{i+1}, \dots, q_{i+l}\}$ defines the i th block of l observations. A MBB sample is then obtained by (i) randomly drawing with replacement from the set of all possible overlapping blocks of size l ; (ii) concentrating the selected blocks and forming a replicated series. Each set of replicated data obtained in this way yields one estimate for the sample mean. The drawing is repeated many times and the block-size-dependent error is approximated by the standard deviation of the bootstrap generated mean values.

It can be shown that in the case of arithmetic mean, σ^2 can be calculated exactly without resampling.²⁶ For a series with n observations, q_i , and k blocks of size l , σ^2 is given by¹⁸

$$\sigma^2 = \frac{1}{kn} \sum_{j=0}^{n-1} \left[\frac{1}{l} \sum_{t=1}^l (q_{j+t} - \langle q \rangle) \right]^2. \quad (14)$$

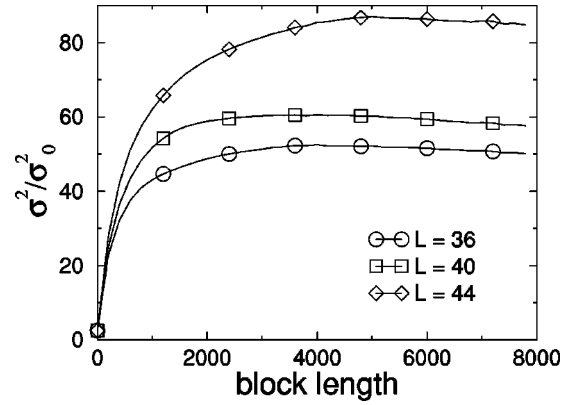


FIG. 7. Moving block bootstrap estimates of the standard errors of the susceptibility as a function of the block length l at criticality for several lattice sizes. The lines are guides to the eye.

The behavior of the ratio σ^2/σ_0^2 is illustrated in Fig. 7 for the susceptibility. The error increases with the block size until it becomes roughly size independent for block length large enough. The maximum value reached by error corresponds to the actual standard error of the mean.

The underlying idea of the MBB method is that if the block length is large enough, observations belonging to different blocks are nearly independent, while the correlation present in observations forming each block is retained.

Having an estimate to σ^2/σ_0^2 , Eq. (13) can be employed to extract τ_{int} . The above outlined procedure was applied for the data of the susceptibility and energy of all lattices. Good agreement was achieved between the estimates of τ_{int} obtained from MBB and by applying directly Eq. (12) for small lattices.

The computed equilibrium relaxation times from both, susceptibility and energy, are plotted in Fig. 8 as obtained from lattices of size $L = 16, 24, 28, \dots, 48$. Notice that, although τ_{int} is quite smaller for the susceptibility, both exhibit the same power-law size dependence. A linear best fit for the energy and susceptibility data yields 3.0 ± 0.1 for the regression coefficient. Therefore, the equilibrium relaxation time scales as $\tau_{int} \propto L^{3.0 \pm 0.1}$. This means that, within the Hand-

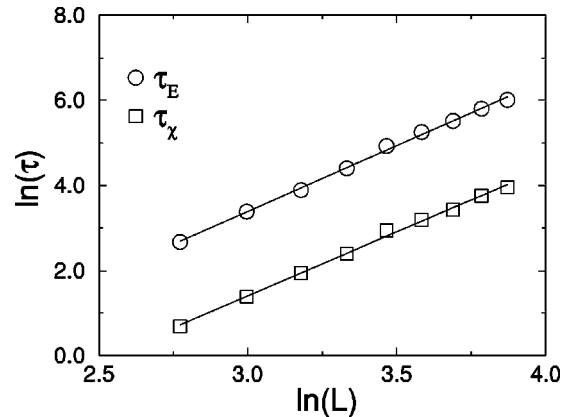


FIG. 8. The equilibrium relaxation time versus linear size L for susceptibility and energy. The error in our estimates of τ_{int} is around 2%. Although, τ_{int} is much smaller for the susceptibility, both quantities scale the same way. The microscopic time scale used is 2000 MCS.

scomb dynamics, the number of Monte Carlo steps per site required to generate uncorrelated diagram configurations at criticality is roughly size independent.

V. CONCLUSIONS

In summary, we performed Monte Carlo simulations of the $S=1/2$ Heisenberg ferromagnet on the simple cubic lattice to investigate the critical relaxation of the Handscomb quantum Monte Carlo method which samples the space of permutation operators appearing in the series expansion of the partition function. Precise estimates of the critical temperature and exponents γ/ν and β/ν were obtained from a phenomenological renormalization group analysis of data from the susceptibility and order parameter. At the critical temperature we measured the equilibrium relaxation time from the time-displaced correlation functions of the susceptibility and energy (small lattices only). For the largest lattices ($L \geq 32$) τ_{int} was estimated through the moving block bootstrap technique. From either susceptibility or energy we obtained that, at criticality, the number of Monte Carlo steps (sampled permutation sequences) required to generate uncorrelated equilibrium diagram configurations scales with the system's volume.

Some care must be taken when estimating the efficiency of the Handscomb method and comparing it with other Monte Carlo prescriptions. First, the phase space sampled within the Handscomb method is not related to any physical space. Therefore, there is no direct relation between the time scales of the Handscomb and the traditional spin-flip dynamics. However, a crude estimate can be drawn by considering that during an elementary Monte Carlo step of the Handscomb dynamics the sites belonging to a particular cycle of permutations have their status updated. The average number

of sites involved in a single Monte Carlo step is then proportional to $1/N \langle a_i^2 \rangle \sim \chi \sim L^{\gamma/\nu}$. Within this reasoning, the average fraction of sites updated in a MCS scales as $L^{\gamma/\nu}/L^d$. Therefore, a time scale which would correspond to a lattice sweep in spin-flip dynamics would be $\tau_0 \sim L^{d-\gamma/\nu}$. In units of this time scale the relaxation time scales as $\tau_{int} \sim \tau_0 L^z$, with $z = 2 \pm 0.1$, which is quite similar to the value of z found for the decoupled cell quantum Monte Carlo and the classical Metropolis dynamics. Although the Handscomb dynamics depicts some characteristics of the classical spin-flip cluster dynamics it has not a similar effect on dealing with the critical slowing down.

It is relevant to mention here that the present Handscomb prescription, which inserts or removes transposition operators at the extremes of the permutation sequence, is the one that provide the simplest algorithm to control the dynamics in the permutation phase space. A natural generalization is to insert and remove operators at random locations within the sequence. This would drastically change its cycle structure with all sites being able to have their status updated on a single step. It would be valuable to estimate the efficiency of such relaxational dynamics at criticality as well as that of other generalizations of the Handscomb prescription as applied to antiferromagnet and large spin models.

ACKNOWLEDGMENTS

We are indebted to D.P. Landau for his suggestions and critical reading of the manuscript. This work was partially supported by CNPq and CAPES (Brazilian research agencies). M.L.L. would like to thank the Physics Department at Universidade Federal de Pernambuco for hospitality during the Summer School 2000 where this work was partially developed.

-
- ¹P. C. Hohenberg and B. I. Halperin, *Rev. Mod. Phys.* **49**, 435 (1977).
²P. Boni and G. Shirane, *Phys. Rev. B* **33**, 3012 (1986).
³P. Boni, M. E. Chen, and G. Shirane, *Phys. Rev. B* **35**, 8449 (1987).
⁴K. Chen and D. P. Landau, *Phys. Rev. B* **49**, 3266 (1994).
⁵D. P. Landau and M. Krech, *J. Phys.: Condens. Matter* **11**, R179 (1999).
⁶J. S. Wang and R. H. Swendsen, *Physica A* **167**, 565 (1990).
⁷P. Peczak and D. P. Landau, *Phys. Rev. B* **47**, 14 260 (1993).
⁸C. Holm and W. Janke, *Phys. Rev. B* **48**, 936 (1993).
⁹C. Holm and W. Janke, *Phys. Rev. Lett.* **78**, 2265 (1997).
¹⁰D. C. Handscomb, *Proc. Cambridge Philos. Soc.* **52**, 594 (1962); **60**, 115 (1964).
¹¹J. W. Lyklema, *Phys. Rev. Lett.* **49**, 88 (1982).
¹²D. H. Lee, J. D. Joannopoulos, and J. W. Negele, *Phys. Rev. B* **30**, 1599 (1984).
¹³I. V. Rojdestvenski, M. L. Lyra, and U. M. S. Costa, *Phys. Rev. B* **56**, 2698 (1997).
¹⁴U. M. S. Costa, I. V. Rojdestvenski, and M. L. Lyra, *Phys. Rev. B* **58**, 2403 (1998).
¹⁵A. W. Sandvik and J. Kurkijärvi, *Phys. Rev. B* **43**, 5950 (1991).
¹⁶M. Suzuki, *Prog. Theor. Phys.* **56**, 1454 (1976); M. Suzuki, S. Miyashita, and A. Kuroda, *ibid.* **58**, 1377 (1977).
¹⁷C. J. Sisson, *Int. J. Mod. Phys. C* **7**, 441 (1996).
¹⁸S. Mignani and R. Rosa, *Comput. Phys. Commun.* **92**, 203 (1995).
¹⁹J. W. Lyklema, in *Monte Carlo Methods in Quantum Problems*, edited by M. H. Kalos (Reidel, Dordrecht, 1984), p. 145.
²⁰Y. C. Chen, H. H. Chen, and F. Lee, *Phys. Rev. B* **43**, 11 082 (1991).
²¹M. P. Nightingale, *Physica A* **83**, 561 (1976).
²²J. Oitmaa and E. Bornilla, *Phys. Rev. B* **53**, 14 228 (1996).
²³K. Chen, A. M. Ferrenberg, and D. P. Landau, *Phys. Rev. B* **48**, 3249 (1993).
²⁴S. Wansleben and D. P. Landau, *Phys. Rev. B* **43**, 6006 (1991).
²⁵K. Binder, Introduction, in *The Monte Carlo Method in Condensed Matter Physics*, edited by K. Binder (Springer-Verlag, Berlin, 1992); A. M. Ferrenberg, D. P. Landau, and K. Binder, *J. Stat. Phys.* **63**, 867 (1991).
²⁶H. R. Künsch, *Ann. Stat.* **17**, 1217 (1989).